

Article

Extreme Precipitation Events During the Wet Season of the South America Monsoon: A Historical Analysis over Three Major Brazilian Watersheds

Aline Araújo de Freitas ^{*}, Vanessa Silveira Barreto Carvalho and Michelle Simões Reboita

Institute of Natural Resources, Federal University of Itajubá (UNIFEI), Itajubá 37500-903, Brazil; vanessa.silveira@unifei.edu.br (V.S.B.C.); reboita@unifei.edu.br (M.S.R.)

* Correspondence: alinefreitas@unifei.edu.br

Abstract: Most of South America, particularly the region between the southern Amazon and southeastern Brazil, as well as a large part of the La Plata Basin, has its climate regulated by the South American Monsoon System. Extreme weather and climate events in these areas have significant socioeconomic impacts. The Madeira, São Francisco, and Paraná river basins, three major watersheds in Brazil, are especially vulnerable to wet and drought periods due to their importance as freshwater ecosystems and sources of water for consumption, energy generation, and agriculture. The scarcity of surface meteorological stations in these basins makes meteorological studies challenging, often using reanalysis and satellite data. This study aims to identify extreme weather (wet) and climate (wet and drought) events during the extended wet season (October to March) from 1980 to 2022 and evaluate the performance of two gridded datasets (CPC and ERA5) to determine which best captures the observed patterns in the Madeira, São Francisco, and Paraná river basins. Wet weather events were identified using the 95th percentile, and wet and drought periods were identified using the Standardized Precipitation Index (SPI) on a 6-month scale. In general, CPC data showed slightly superior performance compared to ERA5 in reproducing statistical measures. For extreme day precipitation, both datasets captured the time series pattern, but CPC better reproduced extreme values and trends. The results also indicate a decrease in wet periods and an increase in drought events. Both datasets performed well, showing they can be used in the absence of station data.

Keywords: extreme rainfall; drought events; Brazilian basins; CPC; ERA5



Citation: Freitas, A.A.d.; Carvalho, V.S.B.; Reboita, M.S. Extreme Precipitation Events During the Wet Season of the South America Monsoon: A Historical Analysis over Three Major Brazilian Watersheds. *Climate* **2024**, *12*, 188. <https://doi.org/10.3390/cli12110188>

Academic Editors: Sudhanshu Sekhar Panda, Ying Ouyang and Johnny M. Grace

Received: 2 October 2024

Revised: 8 November 2024

Accepted: 13 November 2024

Published: 15 November 2024



Copyright: © 2024 by the authors. Licensee MDPI, Basel, Switzerland. This article is an open access article distributed under the terms and conditions of the Creative Commons Attribution (CC BY) license (<https://creativecommons.org/licenses/by/4.0/>).

1. Introduction

Most of South America, between the southern Amazon and southeastern Brazil and a large part of the La Plata Basin, has its climate regulated by a combination of systems and processes that are named the South America Monsoon System (SAMS) [1–6]. The lifecycle of the SAMS is also influenced by several factors such as the complex topography and land uses of the region and the variability in different time scales over the Pacific and Atlantic Oceans, among others [4].

The occurrence of extreme rainfall events leading to floods and rainfall deficits causing droughts has been extensively reported in the SAMS region [7–12], where watersheds are extremely vulnerable to its impacts. Since the present study focuses on extreme events, it is helpful to define what extreme weather and climate events are. Extreme weather events are rare events in a specific location and time of year and extreme climate events are occurrences where a climate variable value exceeds a threshold near the upper or lower limits of observed values and persists for an extended period, such as prolonged droughts or heavy rainfall throughout the season [13].

In Brazil, major watersheds such as the Madeira, São Francisco, and Paraná river basins are extremely vulnerable to extreme weather (wet) and climate (wet and drought) events because of their relevance as freshwater ecosystems and as water sources for human

consumption, energy generation, and agriculture [11,12,14]. Extreme precipitation events, on a weather scale, can lead to flash floods and river flooding [15], while on a climate scale, seasonal meteorological droughts can cause hydrological droughts, which can impact the water supply, energy production, the transportation sector, and water quality [16]. The north of Brazil has been suffering from a lack of rainfall, especially in the Amazon, which has faced drought episodes in recent years, notably in 2005, 2010, 2015–2016, and most recently in 2023/2024 [17,18].

It is also important to highlight that, in areas of South America, meteorological surface stations are scarce [19,20], which leaves important gaps in defining extreme precipitation thresholds, frequency, and patterns. Hence, products such as reanalysis and estimated satellite data are commonly used to provide such information [20], but with no previous validation with some existing stations.

Since extreme precipitation events on both a weather and climate scale can be responsible for biodiversity and economic losses, such as failures in the supply of energy and water for agriculture and navigation, it is important to study the frequency, duration, and intensity of such events. In this framework, the main objective of this study is to describe the occurrence and trends of extreme weather (wet) and climate (wet/drought) events in the Madeira, São Francisco, and Paraná river basins during the extended rainy season of South America (October to March) through observed and grid point datasets: the Climate Prediction Center (CPC) precipitation analysis and ERA5 reanalysis. We also aim to highlight the grid dataset that better represents the observations in the SAMS region. This study is part of the project “Combinando Modelagem Numérica Climática e uso de Aprendizado de Máquina na detecção de extremos climáticos em horizontes subsazonais, sazonais e multi-decadais”, project 88887.688971/2022-00, funded by the Coordination for the Improvement of Higher Education Personnel (CAPES).

2. Materials and Methods

2.1. Study Area

This study focuses on three socio-economically important river basins located in the SAMS region [21–23]: the Madeira River Basin (MRB), the Paraná River Basin (PRB), and the São Francisco River Basin (SFRB) (Figure 1).

2.1.1. Madeira River Basin

The MRB is mainly composed of the Madeira River, which is one of the five rivers with the highest water flow in the world, the longest and most significant tributary of the Amazon River, and one of the main Brazilian rivers [23]. With a hydrographic basin of approximately 1.25 million km², the river runs 3315 km, covering Bolivia (51%), Brazil (42%), and Peru (7%), and is the 17th longest river in the world [23,24]. Originating from the Beni, Mamoré, and Madre de Dios rivers, the river crosses Rondônia and flows into the Amazon [25,26]. The MRB is divided into three regions: Upper, Middle, and Lower Madeira (Figure 1).

Its importance ranges from the subsistence of riverside populations to the regional economy, through the use of its water in agriculture, fishing, industry, waterway transport, and energy production [23–25]. The MRB has a hydroelectric complex, which includes the Jirau and Santo Antônio plants, generating around 3500 MW of energy each, which is subsequently distributed to the Center-West and Southeast regions of Brazil [25,27,28]. The MRB is located in the Amazon biome and features a diverse range of vegetation, including areas of campinaranas, swamps, grasslands, savannas, and upland and floodplain forests [29,30]. The climate present in the basin is equatorial, being hot and humid, with an average precipitation of 1940 mm year⁻¹ and temperatures between 24 and 26 °C [31,32], influenced mainly by the SAMS [2,4,6].

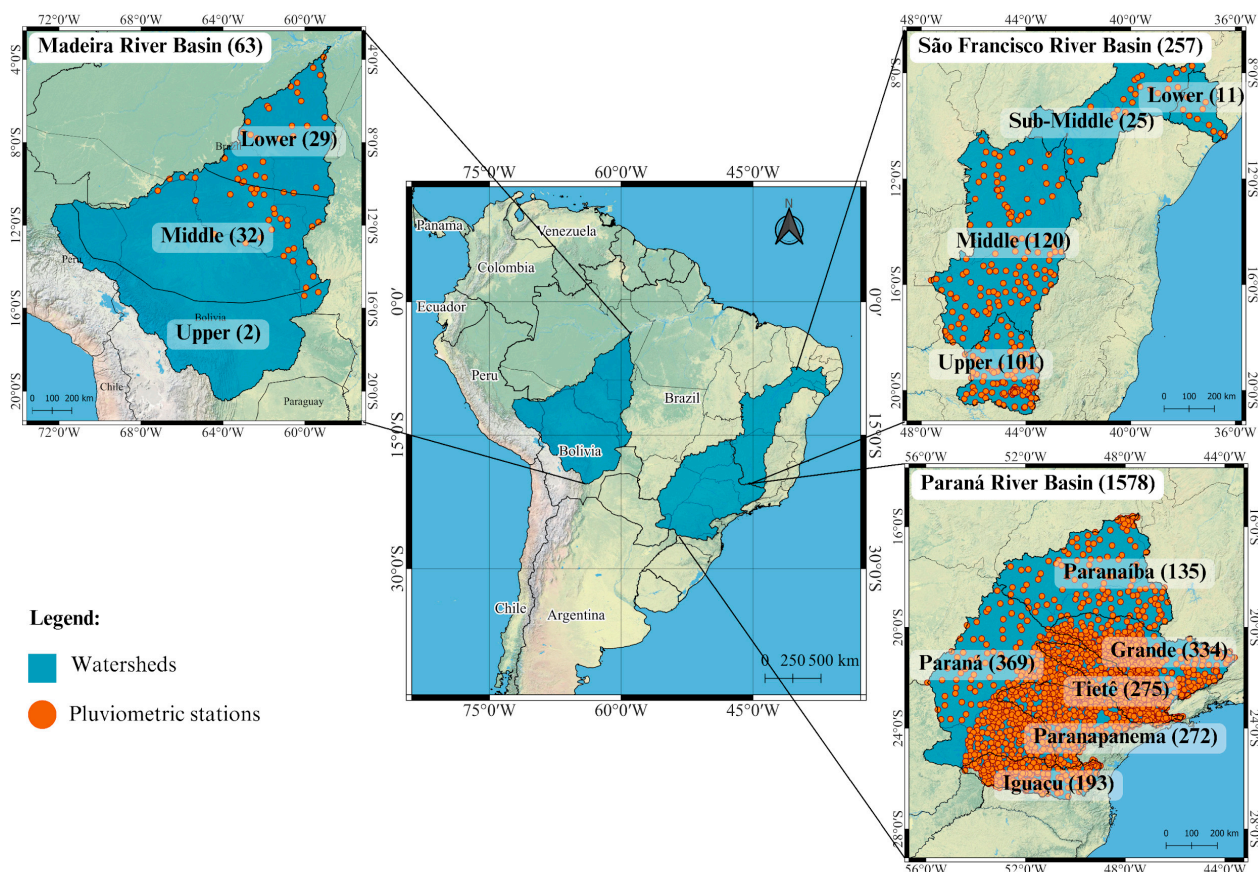


Figure 1. Representation of the study area with a zoom on the basins that were analyzed and the locations of the pluviometric stations used. The number of stations in each basin is also indicated in the figure in parentheses.

2.1.2. Paraná River Basin

The PRB occupies around 10% of the national territory, covering six Brazilian states and the Federal District, with an area of approximately 879,873 km² [22,33]. The PRB is divided into six regions: Paranaíba, Grande, Tietê, Paraná, Paranapanema, and Iguaçú (Figure 1). Located in the most economically developed region of the country, the PRB meets 32% of the national water demand, mainly for irrigation, industrial, and urban use [33,34]. With a population of around 61.4 million inhabitants, the PRB contains 36% of the urban population and produces 45% of the country's GDP [33,34]. It houses important metropolitan regions such as São Paulo, Brasília, and Curitiba [22,33,35]. Furthermore, this region includes the Itaipu Hydroelectric Plant, the largest generator of clean and renewable energy in the world [36,37].

In this basin, the predominant biomes are the Atlantic Forest and the Cerrado [38] and the climatic parameters vary spatially and temporally, affecting water availability in the region. The dominant climate is tropical, except in Paraná and Santa Catarina, where a temperate subtropical climate prevails [33,35]. The SACZ is the main system responsible for rainfall in summer [39,40].

2.1.3. São Francisco River Basin

The SFRB contains an important river, the São Francisco, also known as the National Integration River, which extends for 2863 km from latitude 7°00' S to 21°00' S, crossing six Brazilian states [22,41,42]. The SFRB covers 638,466 km², around 7.5% of the Brazilian territory, and is home to more than 14 million inhabitants [22,34]. The SFRB is divided into four regions [21], Upper, Middle, Sub-Middle, and Lower São Francisco (Figure 1), and stands out for its energy generation potential, with hydroelectric plants such as Três Marias,

Sobradinho, Paulo Afonso, Itaparica, and Xingó, and its water supply for the population, navigation, fishing, agriculture, and basic sanitation [43].

Fragments of biomes such as Cerrado, Caatinga, and Atlantic Forest are found in this basin. Furthermore, due to its territorial extension, its climate varies from hot and humid tropical to semi-arid, influenced by systems such as SACZ [39,40,44] in tUpper and Middle São Francisco and the Intertropical Convergence Zone (ITCZ) [45] in Sub-Middle and Lower São Francisco.

2.2. Data

Daily rainfall data registered between 1980 and 2022 from 1898 pluviometric stations of the National Water and Basic Sanitation Agency (ANA; <https://www.snirh.gov.br/hidroweb/serieshistoricas>, accessed on 10 June 2024) and located in the MRB, PRB, and SFRB were used in this study (Figure 1). However, only sites with at least 7300 days of valid observations (approximately 20 years of data) were considered. ANA data were classified according to consistency: level 1 included pre-analyzed data, used in this study, while level 2 comprised raw data.

Daily rainfall data from the Gauge-Based Analysis of Global Daily Precipitation (CPC) [46,47] generated by the National Oceanic and Atmospheric Administration/Climate Prediction Center (NOAA/CPC) and reanalysis data from ERA5 [48], provided by the European Center for Medium-Range Weather Forecasts (ECMWF), from 1980 to 2022, were also used. CPC analysis has a horizontal spatial resolution of 0.5° and combines data from surface observations of approximately 30,000 sites from around the world, creating a unified, high-quality dataset. ERA5 reanalysis has a 0.25° horizontal spatial resolution and combines model data and global observations to create a complete and consistent dataset, based on the laws of physics.

The flowchart below summarizes all the analyses performed (Figure 2), which will be described in more detail in the following sections.

Extreme weather (wet) and climate (wet/drought) events in the Madeira, São Francisco, and Paraná

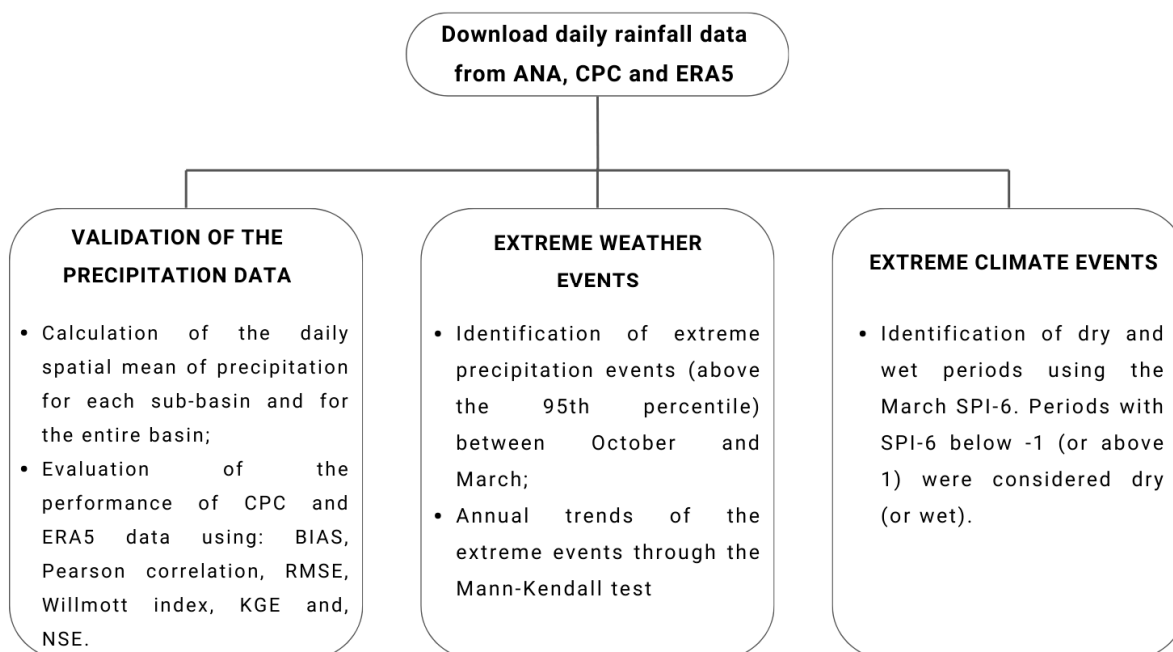


Figure 2. Flowchart summarizing the steps of the analyses performed in this article.

2.3. Validation of the Precipitation Data

Since we aimed to conduct an integrated study of each sub-basin and the basins as a whole, the precipitation spatial average for each sub-basin and the entire basin was initially calculated for each day of the study period and each dataset (CPC, ERA5, and rain-gauge stations). To delimitate the sub-basin and basin areas, the shapefiles provided by ANA were used. Then, to evaluate the performance of CPC analysis and ERA5 reanalysis in the study region, we compared the daily time series obtained with the averaged area with those from rain-gauge stations through a set of statistical measures: mean error (BIAS) [49], Pearson correlation coefficient [50,51], root mean square error (RMSE) [49,51,52], Willmott Index [53,54], Kling–Gupta efficiency coefficient (KGE) [55,56], and Nash–Sutcliffe efficiency (NSE) [57,58].

2.4. Extreme Weather Events

The time series (ANA, CPC, and ERA5) obtained with the methodology from Section 2.3 were used to identify extreme weather events. Daily rainfall extremes occur when the daily precipitation values exceed the 95th percentile (P95), calculated considering only rainfall values above 1 mm within the months of the extended rainy season (from October to March). The number of days per year with precipitation values over the threshold of the 95th percentile was calculated. Following this, the Sun's slope was computed and the Mann–Kendall test [51] was applied to verify the statistical significance (at 0.05 level) of the trends related to the frequency of occurrence of precipitation extremes.

2.5. Extreme Climate Events

Drought and wet periods were identified through the Standardized Precipitation Index (SPI), calculated considering the average time series of the entire basins for all datasets (ANA, CPC, and ERA5). The SPI is an index that only uses historical precipitation series to identify drought and wet periods [59]. It was developed by McKee et al. [60] and has the advantage of being able to be calculated for different time scales, and it is recommended by WMO [61]. In this study, the SPI-6 from March, which refers to precipitation between October (of the previous year) to March, was analyzed. The choice of the March SPI-6 was made based on the desire to evaluate the extended rainy season of South America, in order to check seasonal drought and wet events in the basins during the rainiest months, and to verify which database (CPC or ERA5) has more similarity with observations. Periods in which the March SPI-6 was less (more) than -1 (1) were considered as drought (wet) episodes, the value at which a drought (wet) event begins, according to the SPI classification developed by McKee et al. [60].

3. Results and Discussion

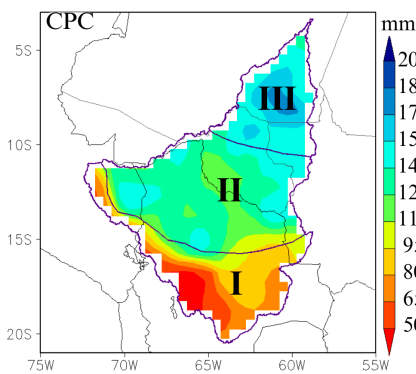
3.1. Basic Statistical Analysis

Although our main focus is on the representation of extreme weather and climate events by CPC and ERA5, here we also present the performance of these grid datasets in reproducing the basic climatology of each subbasin. For the MRB, both datasets (CPC and ERA5) indicate higher precipitation volumes in the northern portion of the basin, where the Lower Madeira (III) region is located, which includes the Madeira river hydroelectric complex, comprising the Jirau and Santo Antônio plants. Higher rainfall is also observed in the western region, near the borders of the Upper (I) and Middle Madeira (II) regions (Figure 3a,b). The southern part of the basin, particularly in the Upper Madeira (I) region, shows lower accumulated rainfall rates, consistent with Vergasta et al. [62], and this subregion presents the greatest discrepancies between the CPC and ERA5, with the CPC indicating low precipitation accumulations throughout the region, while ERA5 shows low values only in the southern part, with some areas in the north accumulating more than 2000 mm. Regarding monthly averages, while CPC tends to underestimate the ANA observations, particularly during the rainy season, ERA5 shows more subtle differences when compared to observations (Figure 3d). This pattern shifts during the driest periods,

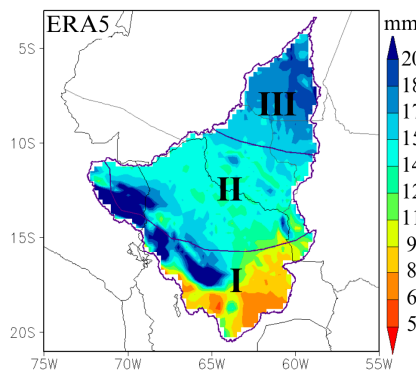
with CPC data aligning more closely with observations, while ERA5 tends to overestimate precipitation in the basin, as also observed by Liu et al. [63], who identified this same tendency for overestimation in relation to monthly precipitation in the Amazon basin region. The statistical results calculated from monthly precipitation data revealed smaller bias for ERA5; however, there were no large differences in other statistical parameters computed for CPC and ERA5, respectively (Figure 3c).

MADEIRA

(a) Climatology of accumulated precipitation during the rainy season (Oct–Mar)



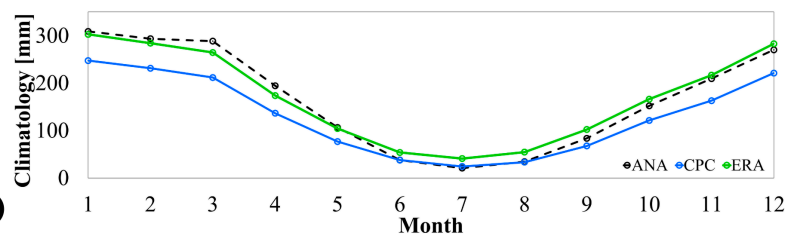
(b)



(c)

Statistics Madeira	CPC	ERA
BIAS	-1.17	0.13
Pearson	0.78	0.70
RMSE	3.29	3.69
Willmott Index	0.86	0.83
KGE	0.65	0.70
NSE	0.55	0.43

(d)



(e)

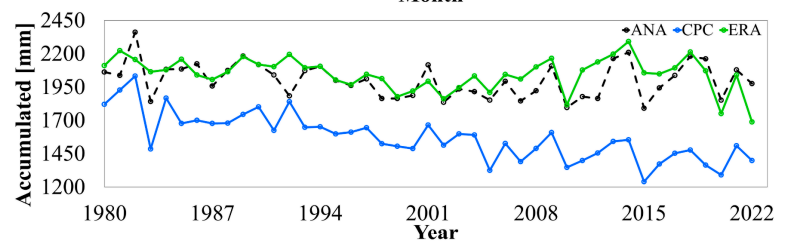


Figure 3. Analysis for the MRB: climatology of accumulated precipitation for the rainy season (October to March) for (a) CPC and (b) ERA5; (c) statistical analysis based on daily data; (d) monthly climatology; and (e) annual accumulation. In (d,e), the ERA5 database is indicated in green, the CPC is indicated in blue, and the observations are shown in black. Regions I, II and III indicate the Upper, Middle and Lower Madeira regions, respectively.

To improve understanding, especially in the Upper Madeira region, where there are few meteorological stations available, two-point comparisons were added (Figure 4). The results show that the CPC model outperforms ERA in both locations in Upper Madeira (1559000 and 1560000). CPC presents lower errors (BIAS and RMSE) and better correlations (Pearson), in addition to greater agreement with observations, reflected in metrics such as the Willmott Index, KGE, and NSE. The monthly climatology and annual accumulated precipitation curves indicate that CPC more accurately captures the seasonal and interannual variability of precipitation, while ERA presents greater deviations, especially in correlation and mean square error.

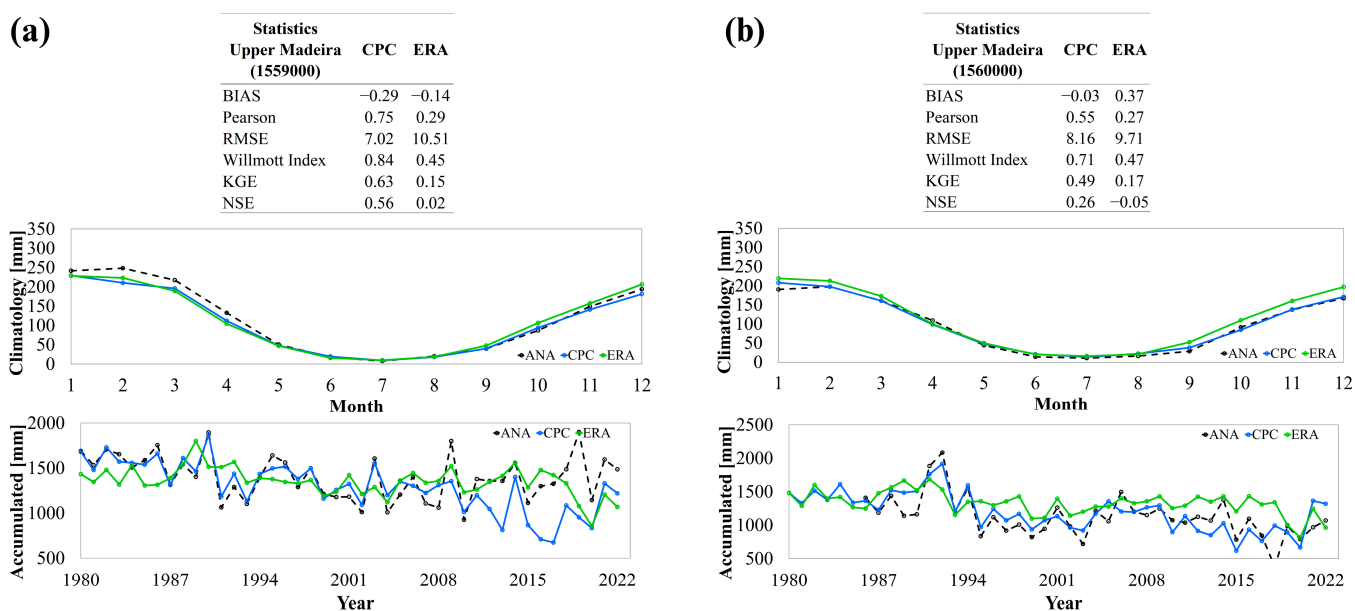


Figure 4. Statistical analysis based on daily data, monthly climatology, and annual accumulation for 2 stations in Upper Madeira: (a) 1559000 and (b) 1560000. The ERA5 database is indicated in green, the CPC is indicated in blue, and the observations are shown in black.

The spatial patterns of precipitation provided by CPC and ERA5 are similar in the PRB (Figure 5a,b). The highest rainfall values are concentrated in the northern (I and II) and southern (VI) extremities of the basin, as also shown by Rafee et al. [64] and Freitas et al. [12]. In the southern part of the region (VI), the Itaipu Power Plant is present—the largest global generator of clean and renewable energy [65]. Despite CPC slightly underestimating precipitation data (negative bias), the results indicate that CPC performs better than ERA5 across this entire basin (Figure 5c). This good performance, albeit with a slight underestimation of the CPC data, was also observed by Cardoso and Quadro [66], who evaluated precipitation in the southern region of Brazil, where a large part of the basin is located.

Due to its vast latitudinal extension, precipitation in the SFRB exhibits higher rainfall values concentrated in the southern sector of the basin (I and II) and lower rainfall values in the Sub-Middle (III) to Lower (IV) São Francisco regions (Figure 6a,b), as also shown by Freitas et al. [11]. The Brazilian semi-arid region is located in subregions III and IV, and the water demand here is greater than the supply, which generates socioeconomic impacts [67,68]. CPC and ERA5 indicate that the monthly and annual average have similar patterns to the observation, although both datasets underestimate precipitation values (Figure 6d,e). The statistical analysis shows that, although closely matched, CPC has superior performance (Figure 6c). Overall, both datasets exhibit high correlation and low bias, with agreement with ANA, especially notable for the CPC database. Torres et al. [69], when evaluating different databases with regard to the SFRB, also identified good performance of CPC data in this region.

In general, for the three basins, both datasets show strong correlation coefficients, low error (RMSE), and high agreement values with the ANA data, indicating good performance (Willmott Index, KGE, and NSE). However, the CPC results stand out, especially in the PRB, demonstrating superior performance compared to the other datasets.

PARANÁ

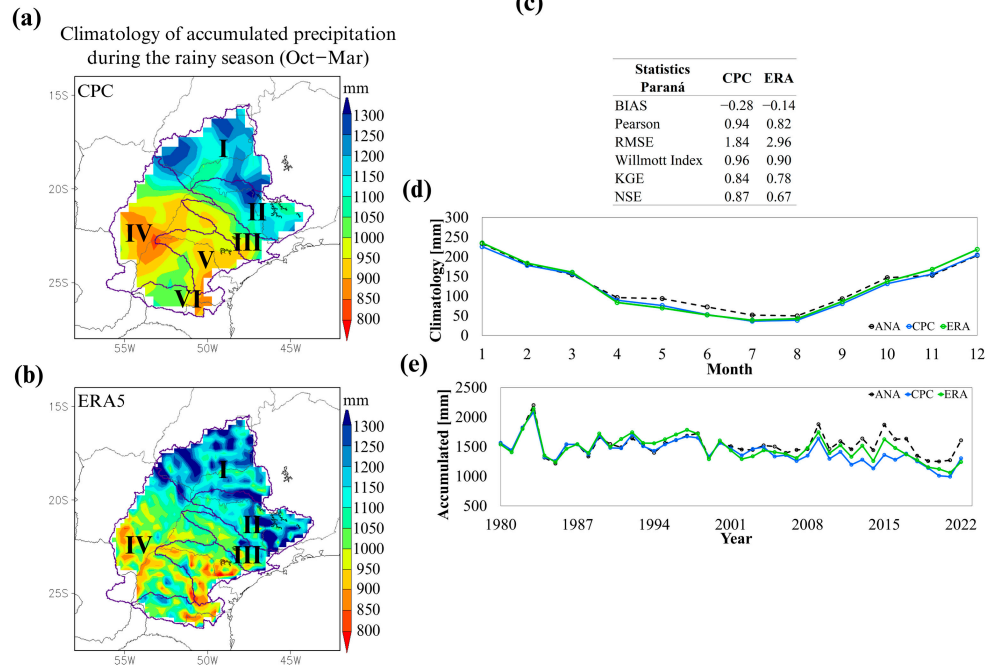


Figure 5. Analysis for the PRB: climatology of accumulated precipitation for the rainy season (October to March) for (a) CPC and (b) ERA5; (c) statistical analysis based on daily data; (d) monthly climatology; and (e) annual accumulation. In (d,e), the ERA5 database is indicated in green, the CPC is indicated in blue, and the observations are shown in black. Regions I, II, III, IV, V, and VI indicate the Paranaíba, Grande, Tietê, Paraná, Parapanema, and Iguaçu regions.

SÃO FRANCISCO

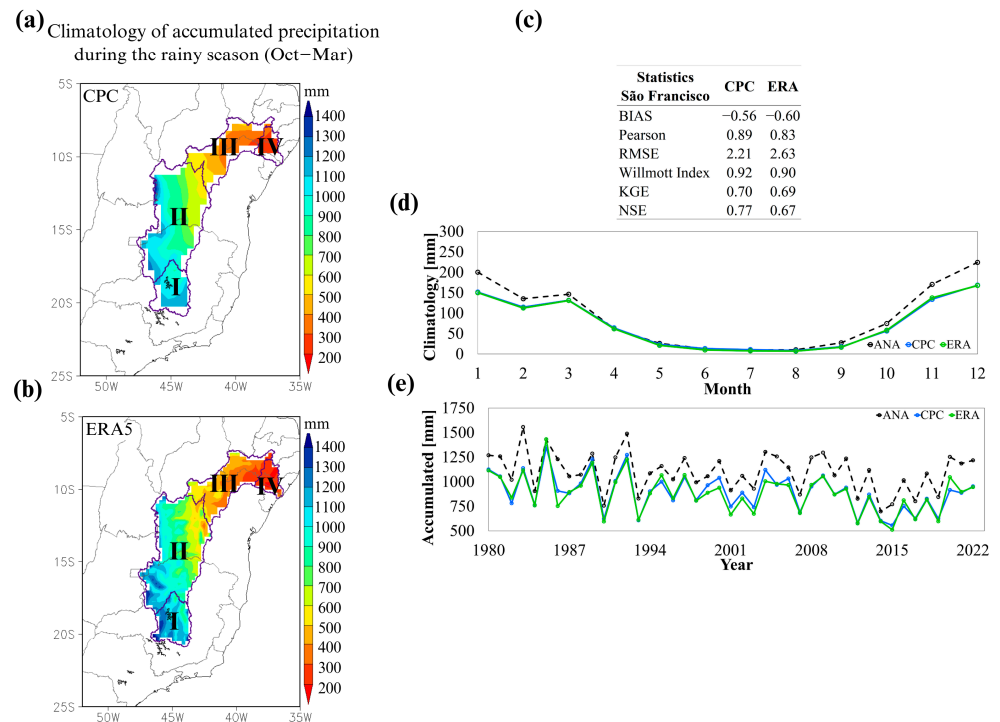


Figure 6. Analysis for the SFRB: climatology of accumulated precipitation for the rainy season (October to March) for (a) CPC and (b) ERA5; (c) statistical analysis based on daily data; (d) monthly climatology; and (e) annual accumulation.

climatology; and (e) annual accumulation. In (d,e), the ERA5 database is indicated in green, the CPC is indicated in blue, and the observations are shown in black. Regions I, II, III, and IV indicate the Upper, Middle, Sub-Middle, and Lower São Francisco regions.

3.2. Extreme Daily Precipitation Events and Trend Analysis

The occurrence of extreme rainfall events was assessed by comparing daily precipitation data (averaged within each subregion of the basin) during the extended rainy season with the 95th percentile values obtained from the time series (ANA, CPC, and ERA5). Except for the Upper Madeira region, which had a limited number of stations available, all other regions showed consistent P95 values across the different datasets (Figure 7), with observations presenting a slightly higher value.

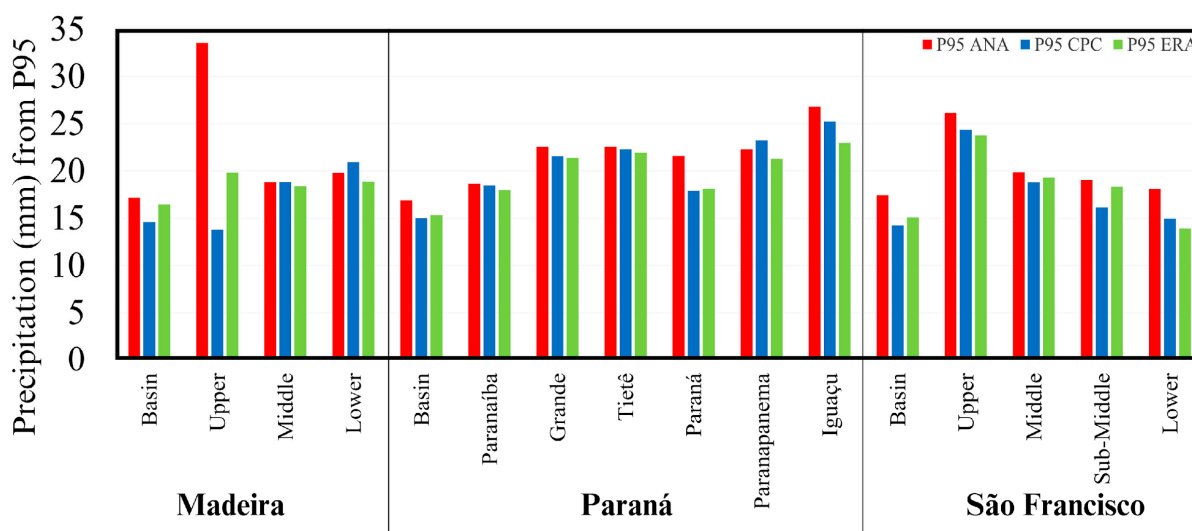


Figure 7. P95 values (precipitation in mm) identified by the ANA, CPC, and ERA5 datasets considering the average in the basins and for each of the subregions. The ERA5 database is indicated in green, the CPC in blue and the observations are shown in red.

The occurrence of extreme events in the MRB (Figure 8a) exhibits a similar average across the analyzed period (1980–2022) in most subregions, except for Upper Madeira, which has only two rain gauges. In the Upper Madeira region, the CPC underestimates the number of extreme events, whereas ERA5 overestimates it. For instance, the years 2007 and 2008 were marked by flood events in this region, leading to significant economic impacts and numerous fatalities [70]. During these years, both CPC and ERA5 recorded extreme precipitation events above the average (Figure 8d). However, ANA data did not indicate a trend, likely due to the limited number of rain gauges in this region. Overall, in the MRB, ANA indicates a decreasing trend in the number of days with extreme rainfall events across the entire basin, with statistical significance in almost every region except Middle Madeira (Table 1). The CPC results corroborate those obtained from ANA data, although they do not show statistical significance. On the other hand, ERA5 indicates a significant increasing trend in the number of occurrences in almost the entire basin. Espinoza et al. [71] also identified a downward trend in the annual frequency of rainy days (precipitation greater than 10 mm) in the period from 1981 to 2009 in the region where the MRB is located, more specifically in the Bolivian Amazon, in the south of the Brazilian Amazon, and in the border area between Peru, Colombia, and Brazil.

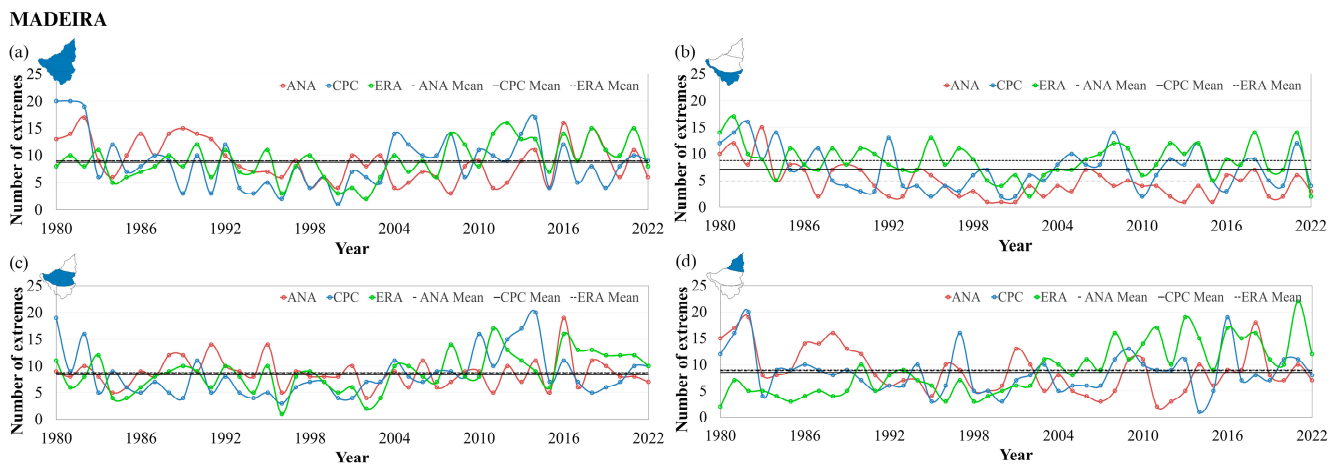


Figure 8. Number of days with extreme precipitation higher than P95 identified by the ANA, CPC, and ERA5 datasets in the MRB regions between 1980 and 2022: (a) entire basin; (b) Upper; (c) Middle; and (d) Lower. In some figures, the means of the datasets are quite close, which causes the black line representing the average to appear as a single line. The ERA5 database is indicated in green, the CPC is indicated in blue, and the observations are shown in red.

Table 1. Trends (increase represented by the letter I and decrease by D) and statistical significance obtained with Mann–Kendall analysis of the different datasets (ANA, CPC, and ERA5), considering the entire basin and the subregions, from 1980 and 2022. Significant trends occur when *p*-value is lower than 0.05.

Region	Mann–Kendall								
	ANA			CPC			ERA5		
	Trend	<i>p</i> -Value	Significant	Trend	<i>p</i> -Value	Significant	Trend	<i>p</i> -Value	Significant
Madeira									
Basin	D	0.0444	Yes	D	0.9413	No	I	0.0189	Yes
Upper	D	0.0052	Yes	D	0.4058	No	D	0.4294	No
Middle	D	0.5604	No	I	0.0795	No	I	0.0068	Yes
Lower	D	0.0143	Yes	D	0.9161	No	I	0.0000	Yes
Paraná									
Basin	D	0.0579	No	D	0.0009	Yes	D	0.0686	No
Paranaíba	D	0.0840	No	D	0.0003	Yes	I	0.8580	No
Grande	D	0.0027	Yes	D	0.0003	Yes	D	0.1280	No
Tietê	D	0.0044	Yes	D	0.0009	Yes	D	0.6265	No
Paraná	I	0.0472	Yes	I	0.1741	No	I	0.8159	No
Parapanema	D	0.3367	No	D	0.7502	No	D	0.3358	No
Iguaçu	D	0.5185	No	D	0.3259	No	I	0.5330	No
São Francisco									
Basin	D	0.0354	Yes	D	0.0668	No	D	0.3306	No
Upper	D	0.1456	No	D	0.0106	Yes	D	0.3067	No
Middle	D	0.0920	No	D	0.2510	No	D	0.6578	No
Sub-Middle	D	0.3559	No	I	0.1625	No	D	0.2238	No
Lower	D	0.8805	No	I	0.0637	No	D	0.3760	No

The average number of extreme events identified through the CPC and ERA5 in the PRB was closely aligned (Figure 9a). Additionally, the evolution in the frequency of extreme rainfall events over the years follows a consistent pattern, albeit with occasional discrepancies where ANA data were either underestimated or overestimated. Across most areas of the basin, notable peaks occurred during the years 1982/1983 and 1997/1998,

marked by above-average values which resulted in economic and social losses due to floods [72]. Strong El Niño events, associated with the movement of the SACZ to the southeast of Brazil, where most of the PRB is located, were detected in both periods, as identified by Valverde and Marengo [72]. However, during the 2020/2021 period, many subregions experienced values below the average, coinciding with severe drought conditions affecting parts of the basin [12]. Overall, the observations also indicated a decreasing trend in the annual occurrence of extreme rainfall events across almost the entire PRB (Table 1). The northern and northeastern portions (Grande and Tietê) showed a statistically significant decrease (Table 1). However, in the central part of the basin, in the Paraná region, there was a significant increase in the annual occurrence of rainfall events. The CPC trends were found to be very similar to those from ANA, indicating a statistically significant decrease in the number of events both for the basin as a whole and in the northern and northeastern portions (Paranaíba, Grande, and Tietê). However, the ERA5 results showed some differences, with an increase in the number of events in more areas, but without statistical significance. The results from ANA and CPC are consistent with previous studies that analyzed the trend of extremes in the PRB region, which also indicate negative trends in the occurrence of extreme rainfall events in the northern and northeastern portions and positive trends in the central and southern parts of the basin [64,73].

PARANÁ

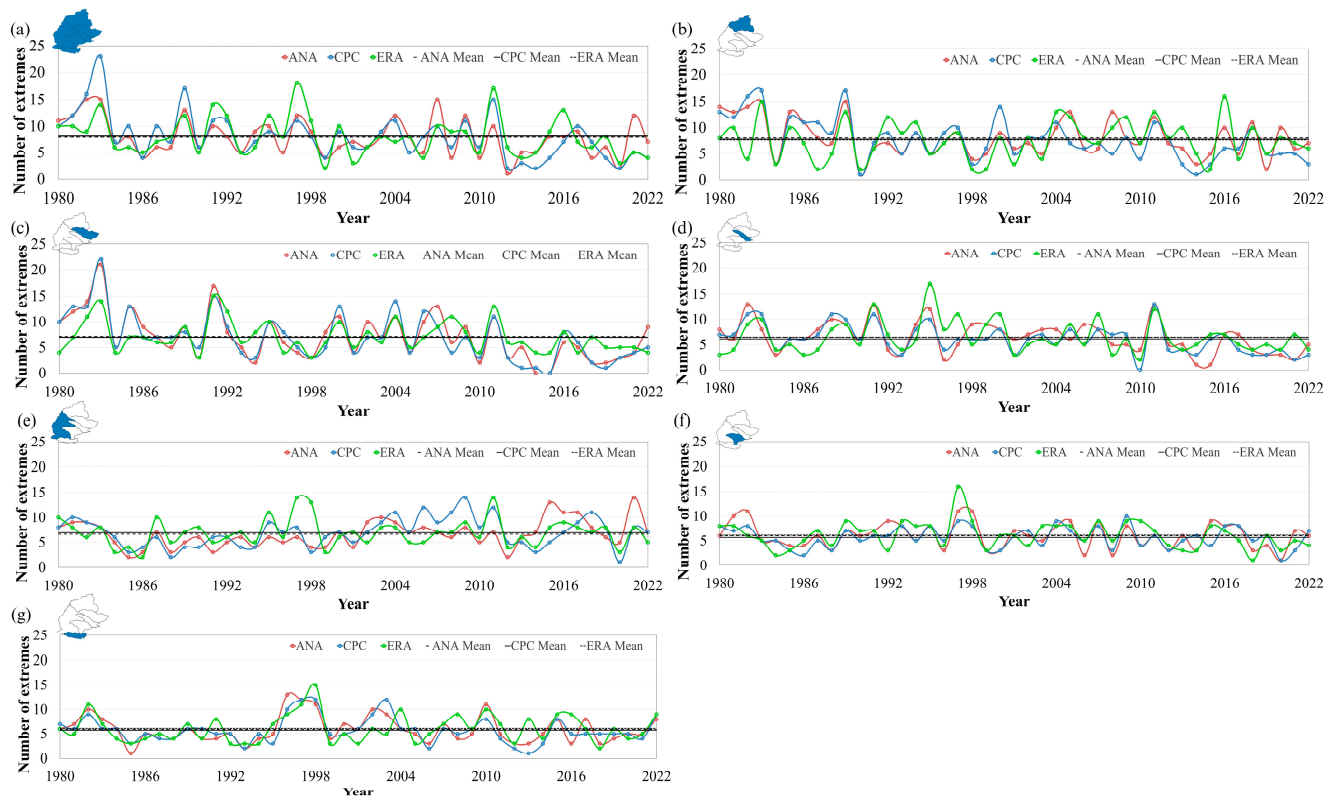


Figure 9. Number of days with extreme precipitation higher than P95 identified by the ANA, CPC, and ERA5 datasets in the PRB regions between 1980 and 2022: (a) entire basin; (b) Paranaíba; (c) Grande; (d) Tietê; (e) Paraná; (f) Parapanema; (g) and Iguaçu. In some figures, the means of the datasets are quite close, which causes the black line representing the average to appear as a single line. The ERA5 database is indicated in green, the CPC is indicated in blue, and the observations are shown in red.

In the SFRB, the average results of extreme rainfall events were consistently similar across all datasets, with minimal variation over time (Figure 10a). The middle São Francisco region exhibited a more uniform pattern in the frequency of extreme events compared

to the other subregions analyzed. For example, 1992 presented the highest number of extreme rainfall events recorded (Figure 10c), coinciding with one of the major floods in the basin [72,74]. Conversely, the SFRB presented the highest number of years without extreme events compared to the MRB and PRB. Specifically, the period 2014/2015 experienced a number of extreme events which was below the average, coinciding with one of the severest droughts in the region [11,75,76]. Overall, ANA data indicated a decreasing trend in the number of extreme rainfall events, with significant decreases across the basin as a whole (Table 1). ERA5 presented results similar to ANA, indicating a decreasing trend in events, but without statistical significance. On the contrary, CPC trends were different, with two regions (Sub-Middle and Lower) showing an increase in the number of extreme events, though not statistically significant. Additionally, the CPC for the Upper São Francisco region, located in southeastern Brazil where the river's source is found, showed a significant decrease in the number of rainfall events. Santos et al. [77] also identified in their study on the semi-arid region of Brazil—where a large part of the SFRB is concentrated—a negative trend in the frequency of extreme events in a large part of the area analyzed in the period from 2001 to 2020.

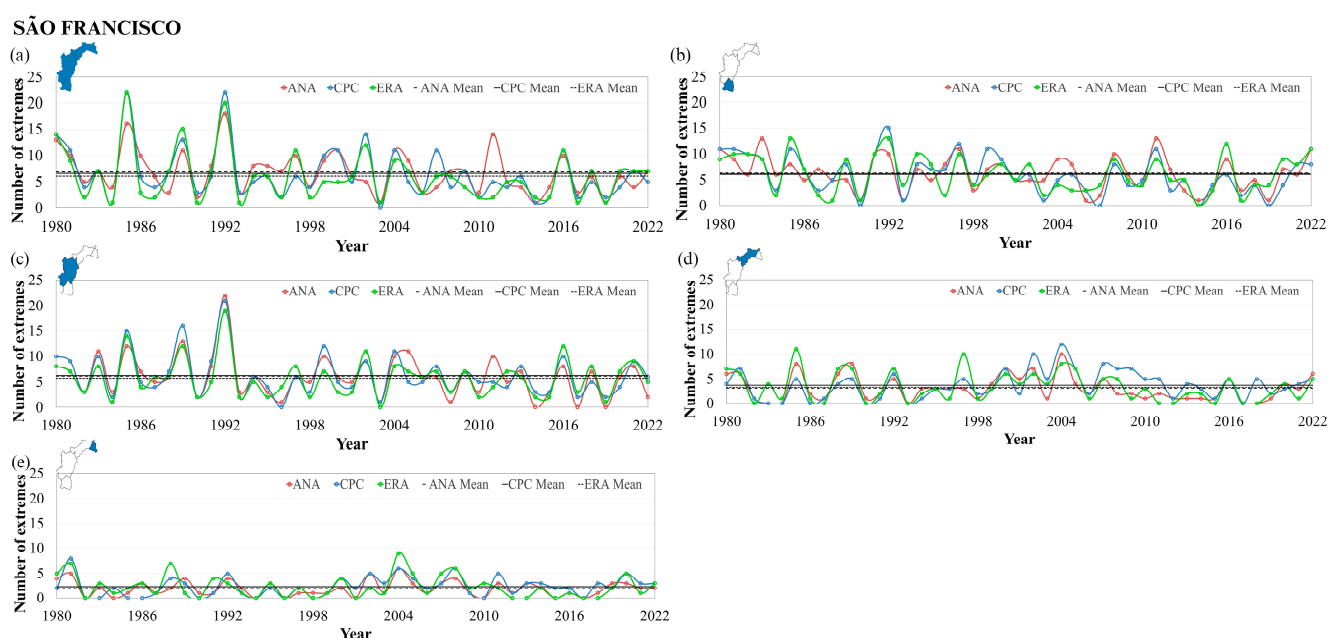


Figure 10. Number of days with extreme precipitation higher than P95 identified by the ANA, CPC, and ERA5 datasets in the SFRB regions between 1980 and 2022: (a) entire basin; (b) Upper; (c) Middle; (d) Sub-Middle; and (e) Lower. In some figures, the means of the datasets are quite close, which causes the black line representing the average to appear as a single line. The ERA5 database is indicated in green, the CPC is indicated in blue, and the observations are shown in red.

3.3. Extreme Climate Events

Climate-related extreme wet and drought events were identified using the SPI-6 from March, which stored the information regarding the extended rainy season. The results revealed a shift in the patterns of occurrence of extreme events across the basin, evident in both datasets (Figure 11). Above-average rainfall events have become less frequent, while drought events have become increasingly common. In the MRB, ANA recorded seven drought episodes and eight wet episodes (Figure 11a). The CPC, in turn, captured six droughts and six wet events, while ERA5 identified six droughts and only five wet periods (Figure 11b,c). Some of the wetter events recorded by ANA are associated with flood years in Porto Velho, a municipality belonging to the MRB, such as 1982, 1984, 1988 and 1997 [78], and these events were more effectively captured by the CPC data (Figure 11b). The year 2014 stands out as a period of unprecedented flooding in both the Brazilian and

Peruvian parts of the basin, which was reflected in the wet conditions observed in the SPI, especially in ERA5 (Figure 11c) [79]. Regarding drought episodes, the literature highlights the years 2005, 2010, 2016, 2020, and 2022 [9,80,81]. The year 2005 was identified as dry by ANA and ERA5, but not by CPC. However, the droughts of 2016, 2020, and 2022 were effectively captured by CPC. The year 2010 was not captured by any dataset, corroborating the observations of Molina-Carpio et al. [82], who also did not identify this period as dry. In general, the ANA and CPC datasets show a similar variation pattern, with more wet episodes at the beginning of the series and more dry episodes at the end. However, ERA5 exhibits an inverse behavior, with an increase in wet events in more recent years.

MADEIRA

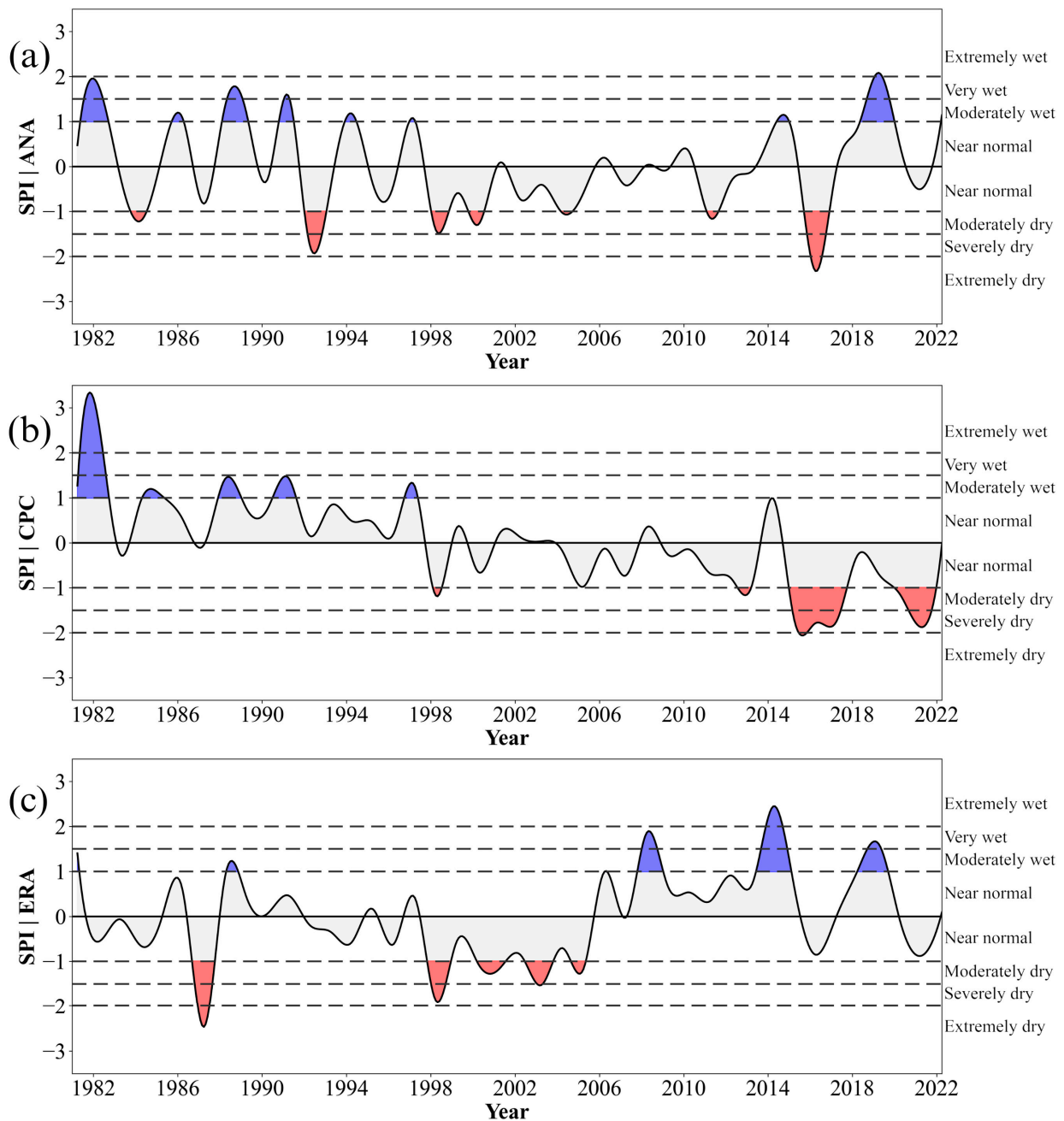


Figure 11. March SPI-6 for the MRB considering the datasets (a) ANA, (b) CPC, and (c) ERA5.

In the case of the PRB, four dry periods and eight wet periods were identified using SPI-6 calculated with ANA data (Figure 12a). Using CPC data, seven dry and five wet episodes were identified, while ERA5 indicated six dry and seven wet periods (Figure 12b,c). In general, the wettest periods occurred at the beginning of the series of all datasets, coinciding with several flood episodes in the basin, mainly between 1983/1984 and during the 1990s [83,84]. The SPI-6 results indicate that the most recent years have been drier in the basin, which is in line with previous findings in the literature [12,85]. Overall, both datasets present consistent SPI results, demonstrating similar behavior throughout the analyzed period.

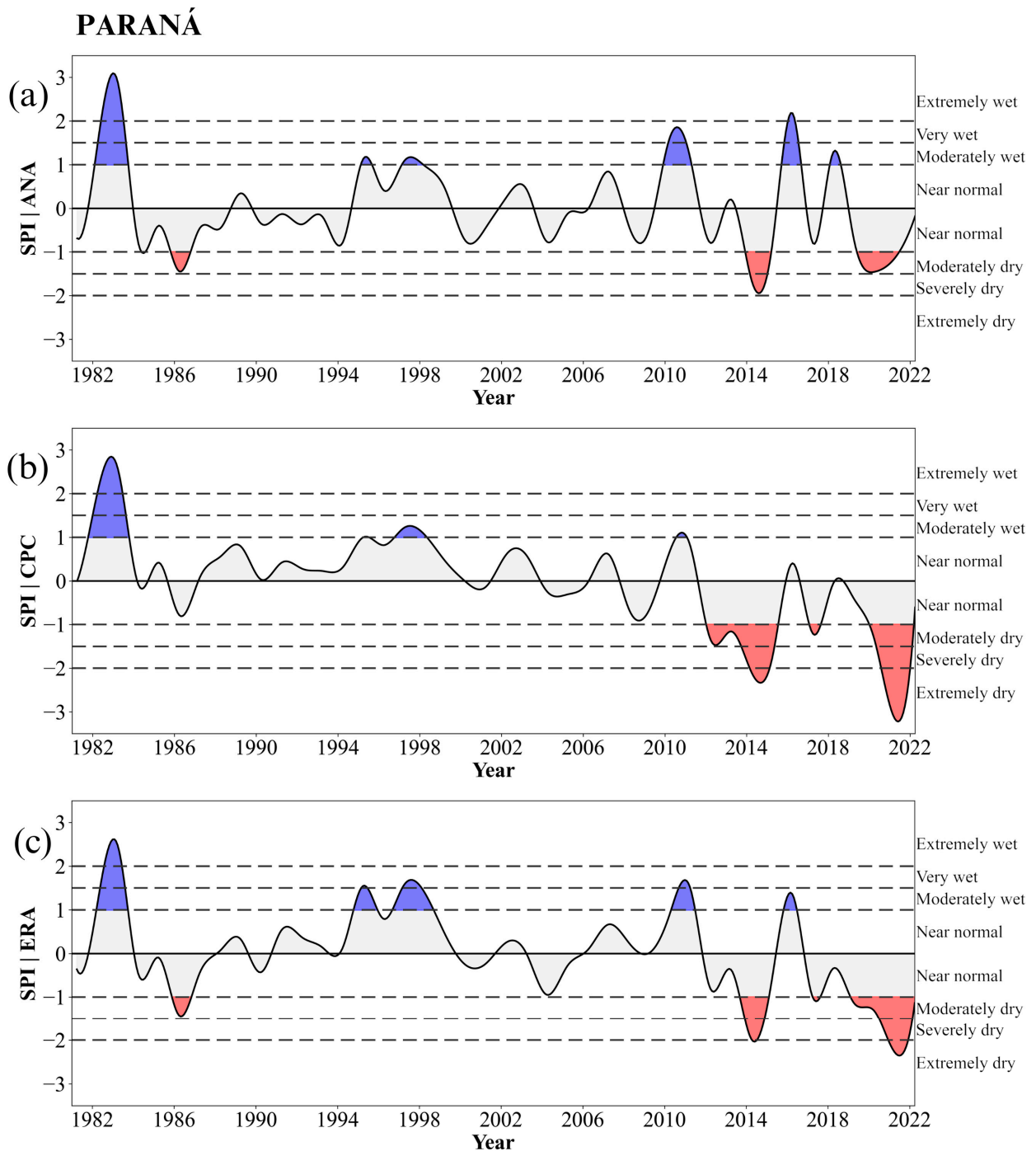


Figure 12. March SPI-6 for the PRB considering the datasets (a) ANA, (b) CPC, and (c) ERA5.

In total, the SPI-6 data from ANA indicate the occurrence of eight dry and seven wet episodes in the SFRB (Figure 13a). The CPC identified six dry and nine wet periods, while ERA5 showed six dry and eight wet periods (Figure 13b,c). As in the PRB, the wettest periods in the SFRB were recorded early in the series in both datasets, coinciding with flood episodes in the basin, such as in 1983, 1992, and 2004 [84,86]. Since 2013, the SFRB has experienced prolonged periods of below-average precipitation, as indicated by the SPI-6 of the analyzed databases, which is in line with reports in the literature [11,76]. Overall, the CPC and ERA5 data effectively identified the behavior of the SPI-6 series in the SFRB during the period from 1980 to 2022.

SÃO FRANCISCO

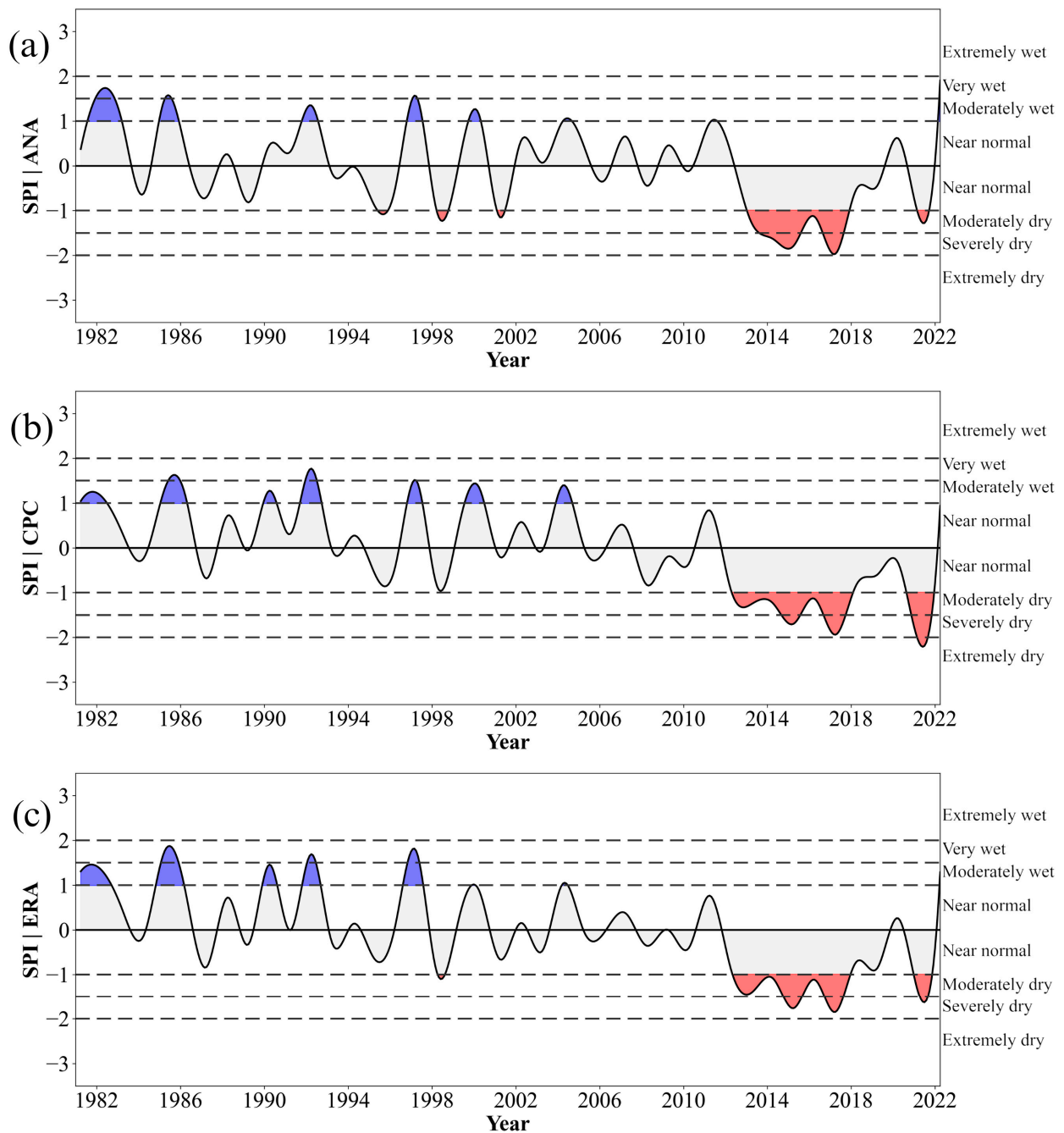


Figure 13. March SPI-6 for the SFRB considering the datasets (a) ANA, (b) CPC, and (c) ERA5.

In general, in the past, drought events in the Amazon region were mainly associated with the warm phase of the El Niño-Southern Oscillation and/or the positive phase of the North Atlantic Oscillation (NAO). The NAO affects the transport of atmospheric moisture to the Amazon, impacting annual rainfall variability [87,88]. In addition, increased deforestation and land use changes in the North and Central regions of Brazil have aggravated these effects, altering local climate dynamics and intensifying the occurrence of dry events in the study areas, especially in the MRB and PRB [89,90]. In the case of the SFRB, the tendency towards desertification is one of the main problems, affecting the hydrological cycle and making the region more arid and susceptible to extreme events [91,92].

4. Conclusions

In this study, an analysis of extreme weather and climate precipitation events during the rainy season was conducted in the MRB, PRB, and SFRB, which belong to the SAMS region. Additionally, the performance of CPC and ERA5 data in identifying the occurrence of these events was evaluated. Statistical analysis of the daily data revealed that the CPC set performed better in all basins analyzed.

The analysis of extreme weather rainfall events showed similar patterns for both datasets in most subregions of the basins. In general, with the exception of Upper Madeira, both datasets captured the pattern of the time series, but CPC better reproduces the extreme values as well as the trend of the data. In the MRB, episodes such as the 2014 flood, which caused losses, were recorded as above-average extreme events by both datasets. In the PRB, CPC and ERA5 records of extremes were aligned, with notable peaks in 1982/1983 and 1997/1998 due to floods that resulted in economic and social losses, and below-average values in 2020/2021 due to a severe drought affecting parts of the basin. In the SFRB, the results were also consistent, with peaks in 1992 coinciding with one of the largest floods in the basin, and periods of low occurrence of extreme events during the severe drought of 2014/2015. Most of the subregions also showed a decreasing trend in the number of identified extreme weather rainfall events between 1980 and 2022.

According to the SPI-6 results, the pattern of extreme climate rainfall and drought events in the basins has changed, with a decrease in the frequency of above-average rainfall events and an increase in droughts. This change has been observed since the mid-1990s in the MRB and PRB and since 2010 in the SFRB. Overall, this change in the pattern of occurrence of extreme weather events was effectively reproduced by both datasets (CPC and ERA5). In the MRB, the extreme drought of 2010 was well represented by the SPI-6 from the datasets. In the PRB, recent SPI-6 data from both datasets indicate an intensification of droughts starting from 2020/2021. In the SFRB, the region has been experiencing prolonged periods of drought since 2013, which are also identified in both datasets. The increase in the occurrence of droughts in recent decades may have significant implications for water availability, agriculture, and biodiversity in the studied basins.

The trends observed in the study basins are expected to persist under climate change scenarios. Studies such as that by [93] indicate drier conditions in the North and Northeast regions of Brazil. In the Amazon, Llopart et al. [94] highlighted that the hydrological cycle is partially affected by the reduction in moisture convergence in the region. These studies serve as important warnings for decision-makers, who need to prepare for problems that are already underway and that may intensify in the future, such as water scarcity and increased occurrence of fires [95,96].

Figure 14 summarizes all analyses performed, indicating which dataset performed best. Overall, the CPC data presented the best statistical results for all basins. Regarding extreme precipitation events, although ERA5 performed better in percentage values, the CPC data identified precipitation extremes better, except for the MRB. For the analysis of drought events and Mann–Kendall trends, both datasets performed well. The lack of meteorological stations in the Upper Madeira region may have negatively influenced the results of the comparison between the datasets. Overall, both datasets performed well, indicating that they can be considered in the absence of station data. It is important to note

the differences in the spatial resolutions of the data, with the CPC having a resolution of 0.5° , while ERA5 has a finer resolution of 0.25° . Furthermore, it is also worth mentioning some limitations of this study, in addition to highlighting the difficulties faced by Latin American researchers, which are mainly associated with the low density of meteorological stations, the quality of the data, which often presents inconsistencies and precision limitations, and the use of interpolation techniques to fill areas with little station coverage, which can result in information that does not always accurately represent real conditions [20].

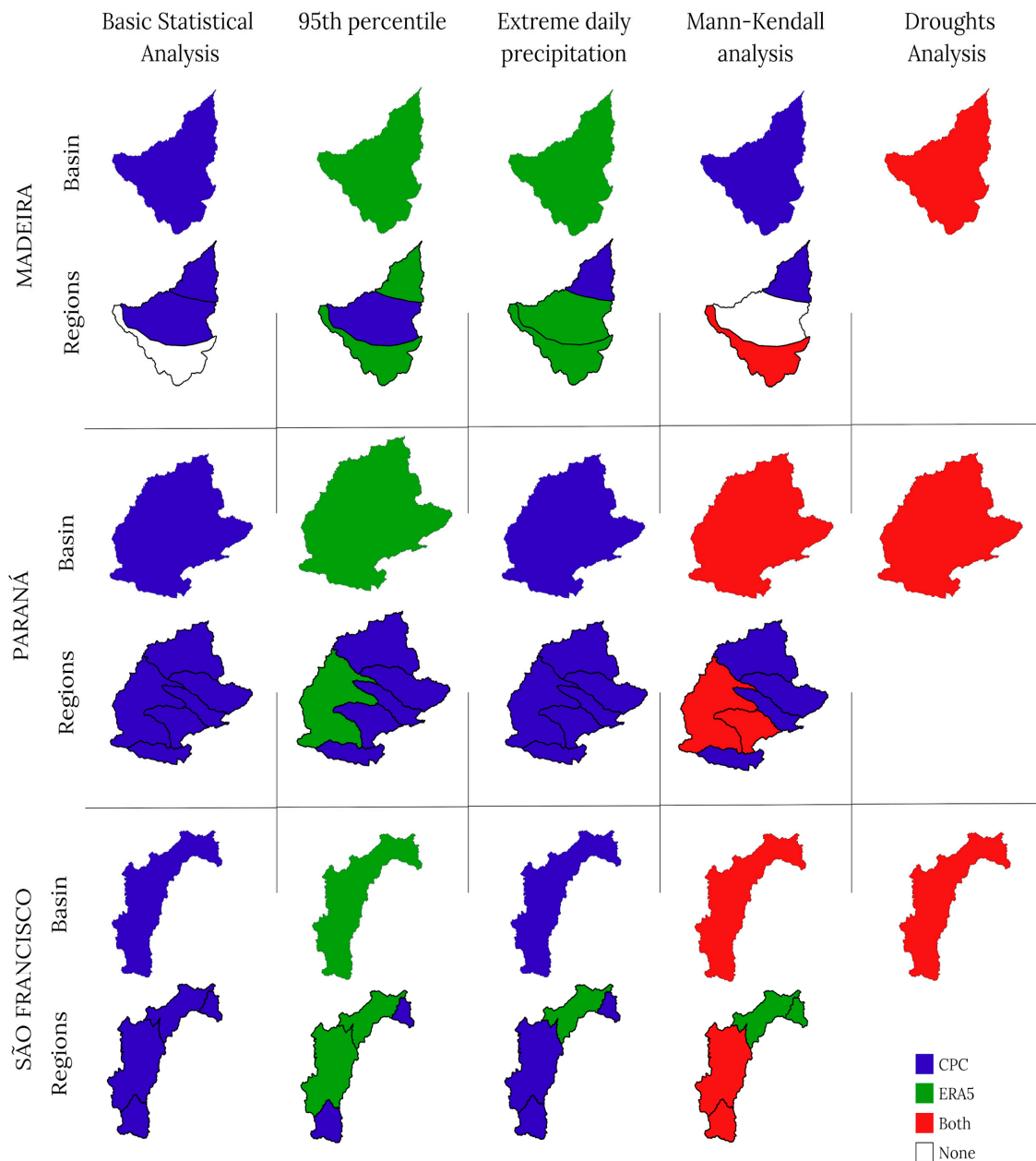


Figure 14. Summary of all analyses performed and which database presented the best results, considering the basin as a whole and the subregions of MRB, PRB, and SFRB.

Author Contributions: Conceptualization, A.A.d.F., V.S.B.C. and M.S.R.; methodology, A.A.d.F., V.S.B.C. and M.S.R.; software, A.A.d.F.; validation, A.A.d.F., V.S.B.C. and M.S.R.; formal analysis, A.A.d.F., V.S.B.C. and M.S.R.; investigation, A.A.d.F., V.S.B.C. and M.S.R.; writing—original draft preparation, A.A.d.F., V.S.B.C. and M.S.R.; writing—review and editing, A.A.d.F., V.S.B.C. and M.S.R.; visualization, A.A.d.F., V.S.B.C. and M.S.R.; supervision, A.A.d.F., V.S.B.C. and M.S.R.; project

administration, A.A.d.F., V.S.B.C. and M.S.R. All authors have read and agreed to the published version of the manuscript.

Funding: This research was funded by the Coordination for the Improvement of Higher Education Personnel (CAPES), grant number 88887.921175/2023-00.

Data Availability Statement: Data are contained within the article.

Acknowledgments: The authors would like to thank the Coordination for the Improvement of Higher Education Personnel (CAPES). We would like to thank ECMWF, CPC, and ANA for providing the data. The authors would like to thank the editor and the anonymous reviewers.

Conflicts of Interest: The authors declare no conflicts of interest.

References

1. Lenters, J.D.; Cook, K.H. Simulation and diagnosis of the regional summertime precipitation climatology of South America. *J. Clim.* **1995**, *8*, 2988–3005. [CrossRef]
2. Zhou, J.; Lau, K.M. Does a monsoon climate exist over South America? *J. Clim.* **1998**, *11*, 1020–1040. [CrossRef]
3. Jones, C. and Carvalho, L.M. Active and break phases in the South American monsoon system. *J. Clim.* **2002**, *15*, 905–914. [CrossRef]
4. Marengo, J.A.; Liebmann, B.; Grimm, A.M.; Misra, V.; Silva Dias, P.L.; Cavalcanti, I.F.A.; Carvalho, L.M.V.; Berbery, E.H.; Ambrizzi, T.; Vera, C.S.; et al. Recent developments on the South American monsoon system. *Int. J. Climatol.* **2012**, *32*, 1–21. [CrossRef]
5. Ferreira, G.W.S.; Reboita, M.S. A new look into the South America precipitation regimes: Observation and forecast. *Atmosphere* **2022**, *13*, 873. [CrossRef]
6. Reboita, M.S.; Teodoro, T.A.; Ferreira, G.W.S.; Souza, C.A. Ciclo de vida do sistema de monção da América do Sul: Clima presente e futuro. *Rev. Bras. Geogr. Fís.* **2022**, *15*, 343–358. [CrossRef]
7. Coelho, C.A.S.; Oliveira, C.P.; Ambrizzi, T.; Reboita, M.S.; Carpenedo, C.B.; Campos, J.L.P.S.; Tomaziello, A.C.N.; Pampuch, L.A.; Custódio, M.S.; Dutra, L.M.M.; et al. The 2014 southeast Brazil austral summer drought: Regional scale mechanisms and teleconnections. *Clim. Dyn.* **2016**, *46*, 3737–3752. [CrossRef]
8. Marengo, J.A.; Williams, E.R.; Alves, L.M.; Soares, W.R.; Rodriguez, D.A. Extreme seasonal climate variations in the Amazon Basin: Droughts and floods. *Interact. Biosph. Atmos. Hum. Land Use Amaz. Basin* **2016**, *227*, 55–76. [CrossRef]
9. Marengo, J.A.; Borma, L.S.; Rodríguez, D.A.; Pinho, P.; Soares, W.R.; Alves, L.M. Recent extremes of drought and flooding in Amazonia: Vulnerabilities and human adaptation. *Am. J. Clim. Change* **2013**, *2*, 87–96. [CrossRef]
10. Santos, E.B.; Freitas, E.D.; Rafee, S.A.A.; Fujita, T.; Rudke, A.P.; Martins, L.D.; Martins, J.A. Spatio-temporal variability of wet and drought events in the Paraná River basin—Brazil and its association with the El Niño—Southern Oscillation phenomenon. *Int. J. Climatol.* **2021**, *41*, 4879–4897. [CrossRef]
11. Freitas, A.A.; Drumond, A.; Carvalho, V.S.B.; Reboita, M.S.; Silva, B.C.; Uvo, C.B. Drought assessment in São Francisco river basin, Brazil: Characterization through SPI and associated anomalous climate patterns. *Atmosphere* **2022**, *13*, 41. [CrossRef]
12. Freitas, A.A.; Reboita, M.S.; Carvalho, V.S.B.; Drumond, A.; Ferraz, S.E.T.; Silva, B.C.; Rocha, R.P. Atmospheric and oceanic patterns associated with extreme drought events over the Paraná Hydrographic Region, Brazil. *Climate* **2023**, *11*, 12. [CrossRef]
13. IPCC. Annex II: Glossary. In *Climate Change 2022: Impacts, Adaptation and Vulnerability. Contribution of Working Group II to the Sixth Assessment Report of the Intergovernmental Panel on Climate Change*; Pörtner, H.-O., Roberts, D.C., Tignor, M., Poloczanska, S.E., Mintenbeck, K., Alegria, A., Craig, M., Langsdorf, S., Löschke, S., Möller, V., et al., Eds.; Cambridge University Press: Cambridge, UK; New York, NY, USA, 2022; pp. 2897–2930.
14. Silva, V.B.; Kousky, V.E. The South American monsoon system: Climatology and variability. *Mod. Climatol.* **2012**, *123*, 152. Available online: https://www.who.edu/cms/files/silva_kousky_217705.pdf (accessed on 17 June 2024).
15. Vu, T.M.; Mishra, A.K. Nonstationary frequency analysis of the recent extreme precipitation events in the United States. *J. Hydrol.* **2019**, *575*, 999–1010. [CrossRef]
16. Van Lanen, H.A.J.; Laaha, G.; Kingston, D.G.; Gauster, T.; Ionita, M.; Vidal, J.P.; Vlnas, R.; Tallaksen, L.M.; Stahl, K.; Hannaford, J.; et al. Hydrology needed to manage droughts: The 2015 European case. *Hydrol. Process.* **2016**, *30*, 3097–3104. [CrossRef]
17. Marengo, J.A.; Tomasella, J.; Alves, L.M.; Soares, W.R.; Rodriguez, D.A. The drought of 2010 in the context of historical droughts in the Amazon region. *Geophys. Res. Lett.* **2011**, *38*, 1–5. [CrossRef]
18. Lima, L.S.; Silva, F.E.O.E.; Dorio Anastácio, P.R.; Kolanski, M.M.D.P.; Pires Pereira, A.C.; Menezes, M.S.R.; Macedo, M.N. Severe droughts reduce river navigability and isolate communities in the Brazilian Amazon. *Commun. Earth Environ.* **2024**, *5*, 370. [CrossRef]
19. Lagos-Zúñiga, M.; Balmaceda-Huarte, R.; Regoto, P.; Torrez, L.; Olmo, M.; Lyra, A.; Pareja-Quispe, D.; Bettolli, M.L. Extreme indices of temperature and precipitation in South America: Trends and intercomparison of regional climate models. *Clim. Dyn.* **2022**, *62*, 4541–4562. [CrossRef]
20. Cavazos, T.; Bettolli, M.L.; Campbell, D.; Sánchez Rodríguez, R.A.; Mycoo, M.; Arias, P.A.; Rivera, J.; Simões Reboita, M.; Gulizia, C.; Hidalgo, H.G.; et al. Challenges for climate change adaptation in Latin America and the Caribbean region. *Front. Clim.* **2024**, *6*, 1392033. [CrossRef]

21. ANA. *Projeto de Gerenciamento Integrado das Atividades Desenvolvidas em Terra na Bacia do Rio São Francisco: Programa de ações estratégicas para o gerenciamento integrado da Bacia do Rio São Francisco e da sua Zona Costeira*; PAE: Brasília, Brazil, 2004; p. 50.
22. ANA. *Conjuntura dos recursos hídricos no Brasil: Regiões hidrográficas brasileiras—Edição Especial*; ANA: Brasília, Brazil, 2015; p. 164.
23. ANA. Madeira. 2024. Available online: <https://www.gov.br/ana/pt-br/sala-de-situacao/rio-madeira/saiba-mais> (accessed on 10 June 2024).
24. CEMADEN. 13/04/2018—Previsão de vazão para bacia do Rio Madeira. 2018. Available online: <http://www2.cemaden.gov.br/13042018-previsao-de-vazao-para-bacia-do-rio-madeira/> (accessed on 10 June 2024).
25. ANA. *Plano estratégico de recursos hídricos dos afluentes da margem direita do rio Amazonas: Resumo executivo/Agência Nacional de Águas*; ANA: Brasília, Brazil, 2012; p. 146.
26. Santo Antônio Energia. Saiba Mais Rio Madeira. 2022. Available online: https://www.santoantonioenergia.com.br/wp-content/uploads/2022/08/02_rio_madeira.pdf (accessed on 10 June 2024).
27. Eletrobras Furnas. Usina de Santo Antônio. 2024. Available online: <https://www.furnas.com.br/subsecao/134/usina-de-santo-antonio?culture=pt> (accessed on 10 June 2024).
28. JIRAU. A estrutura da usina hidrelétrica Jirau. 2024. Available online: <https://www.jirauenergia.com.br/conheca-a-uhe/> (accessed on 10 June 2024).
29. INPA. *Biodiversidade do médio Madeira: Bases científicas para propostas de conservação*; INPA: Manaus, Brazil, 2007; p. 239.
30. Perigolo, N.A.; Medeiros, M.B.; Simon, M.F. Vegetation types of the upper Madeira River in Rondônia, Brazil. *Brittonia* **2017**, *69*, 423–446. [[CrossRef](#)]
31. Muniz, L.S. Análise dos padrões fluviométricos da Bacia do Rio Madeira-Brasil. Master's Thesis, Universidade Federal do Amazonas, Manaus, Brazil, 2013; p. 146. Available online: <https://tede.ufam.edu.br/handle/tede/3961> (accessed on 10 June 2024).
32. Ribeiro Neto, A.; Silva, R.C.V.; Collischonn, W.; Tucci, C.E.M. Simulação na bacia Amazônica com dados limitados: Rio Madeira. *RBRH* **2008**, *13*, 47–58. [[CrossRef](#)]
33. MMA. *Caderno da Região Hidrográfica do Paraná/Ministério do Meio Ambiente*; Secretaria de Recursos Hídricos; MMA: Brasília, Brazil, 2006; p. 122.
34. SNIRH. Atlas Geográfico digital de recursos hídricos do Brasil. 2013. Available online: <https://portal1.snirh.gov.br/atlasrh2013/> (accessed on 17 July 2024).
35. ANA. *Atlas Brasil: Abastecimento urbano de água: Panorama nacional*; ANA: Brasília, Brazil, 2010; p. 72.
36. Itaipu Binacional. *Assegurar o acesso confiável, sustentável, moderno e a preço acessível à energia para todas e todos/Itaipu Binacional*; Central Hidrelétrica de Itaipu: Paraná, Brazil, 2019; p. 56. Available online: https://www.itaipu.gov.br/sites/default/files/af_df/Estudo_de_caso_Itaipu_ODS_7.pdf (accessed on 17 June 2024).
37. Itaipu Binacional. *Relatório Anual Itaipu Binacional 2020*; Central Hidrelétrica de Itaipu: Paraná, Brazil, 2020; p. 132. Available online: https://www.itaipu.gov.br/sites/default/files/af_df/Relatorio_Anual_2020_v2.pdf (accessed on 17 June 2024).
38. Rudke, A.P.; Xavier, A.C.F.; Martins, L.D.; Freitas, E.D.; Uvo, C.B.; Hallak, R.; Souza, R.A.F.; Andreoli, R.V.; Almeida Albuquerque, T.T.; Martins, J.A. Landscape changes over 30 years of intense economic activity in the upper Paraná River basin. *Ecol. Informat.* **2022**, *72*, 101882. [[CrossRef](#)]
39. Reboita, M.S.; Marietto, D.M.G.; Souza, A.; Barbosa, M. Caracterização atmosférica quando da ocorrência de eventos extremos de chuva na região sul de Minas Gerais. *Rev. Bras. Climatol.* **2017**, *21*, 20–37. [[CrossRef](#)]
40. Escobar, G.C.J.; Reboita, M.S. Relationship between daily atmospheric circulation patterns and South Atlantic Convergence Zone (SACZ) events. *AtmÓsfera* **2022**, *35*, 1–25. [[CrossRef](#)]
41. CODEVASF. *Plano Nascente: Plano de preservação e recuperação de nascentes da bacia do rio São Francisco*; IABS: Brasília, Brazil, 2015; p. 129.
42. CBHSF. A Bacia. 2024. Available online: <https://cbhsaofrancisco.org.br/a-bacia/> (accessed on 8 July 2024).
43. IBGE. *Vetores Estruturantes da Dimensão Socioeconômica da Bacia Hidrográfica do Rio São Francisco*; IBGE: Rio de Janeiro, Brazil, 2009; p. 174.
44. Silva, D.F.; Brito, J.I.B. Variabilidade do vento na bacia hidrográfica do rio São Francisco durante a ocorrência da ZCAS. *Ambiência* **2008**, *4*, 221–235. Available online: <https://revistas.unicentro.br/index.php/ambiencia/article/view/164> (accessed on 17 June 2024).
45. Utida, G.; Cruz, F.W.; Etourneau, J.; Bouloubassi, I.; Schefuß, E.; Vuille, M.; Novello, V.F.; Prado, L.F.; Sifeddine, A.; Klein, V.; et al. Tropical South Atlantic influence on Northeastern Brazil precipitation and ITCZ displacement during the past 2300 years. *Sci. Rep.* **2019**, *9*, 1698. [[CrossRef](#)]
46. Chen, M.; Shi, W.; Xie, P.; Silva, V.B.; Kousky, V.E.; Higgins, R.W.; Janowiak, J.E. Assessing objective techniques for gauge-based analyses of global daily precipitation. *J. Geophys. Res. Atmos.* **2008**, *113*, D04110. [[CrossRef](#)]
47. Sun, Q.; Miao, C.; Duan, Q.; Ashouri, H.; Sorooshian, S.; Hsu, K.L. A review of global precipitation data sets: Data sources, estimation, and intercomparisons. *Rev. Geophys.* **2018**, *56*, 79–107. [[CrossRef](#)]
48. Hersbach, H.; Bell, B.; Berrisford, P.; Hirahara, S.; Horányi, A.; Muñoz-Sabater, J.; Nicolas, J.; Peubey, C.; Radu, R.; Schepers, D.; et al. The ERA5 global reanalysis. *Q. J. R. Meteorol. Soc.* **2020**, *146*, 1999–2049. [[CrossRef](#)]
49. Montgomery, D.C.; Jennings, C.L.; Kulahci, M. *Introduction to Time Series Analysis and Forecasting*; John Wiley & Sons: Hoboken, NJ, USA, 2015; p. 671.

50. Hinkle, D.E.; Wiersma, W.; Jurs, S.G. *Applied Statistics for the Behavioral Sciences*; Houghton Mifflin: Boston, MA, USA, 2003; Volume 663, p. 748.
51. Wilks, D.S. *Statistical Methods in the Atmospheric Sciences*, 4th ed.; Elsevier: Amsterdam, The Netherlands, 2019; p. 807.
52. Hallak, R.; Pereira Filho, A.J. Metodologia para análise de desempenho de simulações de sistemas convectivos na região metropolitana de São Paulo com o modelo ARPS: Sensibilidade a variações com os esquemas de advecção e assimilação de dados. *Rev. Bras. Meteorol.* **2011**, *26*, 591–608. [CrossRef]
53. Willmott, C.J. On the validation of models. *Phys. Geogr.* **1981**, *2*, 184–194. [CrossRef]
54. Willmott, C.J.; Robeson, S.M.; Matsuura, K. A refined index of model performance. *Int. J. Climatol.* **2012**, *32*, 2088–2094. [CrossRef]
55. Gupta, H.V.; Kling, H.; Yilmaz, K.K.; Martinez, G.F. Decomposition of the mean squared error and NSE performance criteria: Implications for improving hydrological modelling. *J. Hydrol.* **2009**, *377*, 80–91. [CrossRef]
56. Kling, H.; Fuchs, M.; Paulin, M. Runoff conditions in the upper Danube basin under an ensemble of climate change scenarios. *J. Hydrol.* **2012**, *424*, 264–277. [CrossRef]
57. Nash, J.E.; Sutcliffe, J.V. River flow forecasting through conceptual models part I—A discussion of principles. *J. Hydrol.* **1970**, *10*, 282–290. [CrossRef]
58. Moriasi, D.N.; Arnold, J.G.; Van Liew, M.W.; Bingner, R.L.; Harmel, R.D.; Veith, T.L. Model evaluation guidelines for systematic quantification of accuracy in watershed simulations. *Trans. ASABE* **2007**, *50*, 885–900. [CrossRef]
59. Fernandes, D.S.; Heinemann, A.B.; Paz, R.L.; Amorim, A.O.; Cardoso, A.S. *Índices Para a Quantificação da Seca*; Embrapa Arroz e Feijão-Documents: Colombo, Brazil, 2009; p. 48. Available online: <http://www.infoteca.cnptia.embrapa.br/infoteca/handle/doc/663874> (accessed on 3 July 2024).
60. Mckee, T.B.; Doesken, N.J.; Kleist, J. The relationship of drought frequency and duration to time scales. In Proceedings of the 8th Conference on Applied Climatology, Anaheim, CA, USA, 17–22 January 1993; pp. 179–183.
61. WMO. Standardized Precipitation Index. In *User Guide*; WMO: Geneva, Switzerland, 2012; p. 24.
62. Vergasta, L.A.; Correia, F.W.S.; Chou, S.C.; Nobre, P.; Lyra, A.D.A.; Gomes, W.D.B.; Capistrano, V.; Veiga, J.A.P. Avaliação do Balanço de água na Bacia do Rio Madeira Simulado Pelo Modelo Regional Climático Eta e o Modelo Hidrológico de Grandes Bacias MGB. *Rev. Bras. Meteorol.* **2021**, *36*, 153–169. [CrossRef]
63. Liu, R.; Zhang, X.; Wang, W.; Wang, Y.; Liu, H.; Ma, M.; Tang, G. Global-scale ERA5 product precipitation and temperature evaluation. *Ecol. Indic.* **2024**, *166*, 112481. [CrossRef]
64. Rafee, S.A.A.; Freitas, E.D.; Martins, J.A.; Martins, L.D.; Domingues, L.M.; Nascimento, J.M.; Machado, C.B.; Santos, E.B.; Rudke, A.P.; Fujita, T.; et al. Spatial trends of extreme precipitation events in the Paraná river basin. *J. Appl. Meteorol. Climatol.* **2020**, *59*, 443–454. [CrossRef]
65. Itaipu Binacional. Revista Itaipu Binacional. 2017. Available online: https://www.itaipu.gov.br/sites/default/files/af_df/1702_022_atualizacao_revista_IB_2017_digital_b.pdf (accessed on 17 June 2024).
66. Cardoso, C.S.; Quadro, M.F.L. Análise comparativa de dados de precipitação gerados pelo “Climate Prediction Center–CPC” versus dados observados para o Sul do Brasil. *Rev. Bras. Geogr. FÍS.* **2017**, *10*, 1180–1198. [CrossRef]
67. Correia, R.C.; Kiill, L.H.P.; Moura, M.S.B.; Cunha, T.J.F.; Jesus Júnior, L.A.; Araújo, J.L.P. *A Região Semiárida Brasileira*; Embrapa: Brasília, Brazil, 2011; p. 28. Available online: <https://www.embrapa.br/busca-de-publicacoes/-/publicacao/916891/a-regiao-semiarida-brasileira> (accessed on 17 June 2024).
68. Marengo, J.A.; Alves, L.M.; Beserra, E.A.; Lacerda, F.F. Variabilidade e mudanças climáticas no semiárido brasileiro. *Rec. Hídricos Regiões Áridas SemiÁridas* **2011**, *1*, 385–422. Available online: <https://www.ccst.inpe.br/publicacao/variabilidade-e-mudancas-climaticas-no-semiarido-brasileiro/> (accessed on 3 July 2024).
69. Torres, F.L.R.; Souza Ferreira, G.W.; Kuki, C.A.C.; Vasconcellos, B.T.C.; Freitas, A.A.; Nascimento Silva, P.; Souza, C.A.; Reboita, M.S. Validação de diferentes bases de dados de precipitação nas bacias hidrográficas do Sapucaí e São Francisco. *Rev. Bras. Climatol.* **2020**, *27*, 368–404. [CrossRef]
70. Ovando, A.; Tomasella, J.; Rodriguez, D.A.; Martinez, J.M.; Siqueira-Junior, J.L.; Pinto, G.L.N.; Passy, P.; Vauchel, P.; Noriega, L.; von Randow, C. Extreme flood events in the Bolivian Amazon wetlands. *J. Hydrol. Reg. Stud.* **2016**, *5*, 293–308. [CrossRef]
71. Espinoza, J.C.; Ronchail, J.; Marengo, J.A.; Segura, H. Contrasting North–South changes in Amazon wet-day and dry-day frequency and related atmospheric features (1981–2017). *Clim. Dyn.* **2019**, *52*, 5413–5430. [CrossRef]
72. Valverde, M.C.; Marengo, J.A. Extreme rainfall indices in the hydrographic basins of Brazil. *Open J. Mod. Hydrol.* **2014**, *4*, 10–26. [CrossRef]
73. Cerón, W.L.; Kayano, M.T.; Andreoli, R.V.; Avila-Diaz, A.; Ayes, I.; Freitas, E.D.; Martins, J.A.; Souza, R.A. Recent intensification of extreme precipitation events in the La Plata Basin in Southern South America (1981–2018). *Atmos. Res.* **2021**, *249*, 105299. [CrossRef]
74. CBHSF. *Plano de recursos hídricos da bacia hidrográfica do rio São Francisco*; CBHSF: Bahia, Brazil, 2004; p. 337.
75. Marengo, J.A.; Cunha, A.P.; Alves, L.M. A seca de 2012–15 no semiárido do Nordeste do Brasil no contexto histórico. *Rev. Climanálise* **2016**, *3*, 49–54. Available online: <http://climanalise.cptec.inpe.br/~rclimanl/revista/pdf/30anos/marengoetal.pdf> (accessed on 3 July 2024).
76. Cunha, A.P.M.A.; Zeri, M.; Deusdará Leal, K.; Costa, L.; Cuartas, L.A.; Marengo, J.A.; Tomasella, J.; Vieira, R.M.; Barbosa, A.A.; Cunningham, C.; et al. Extreme drought events over Brazil from 2011 to 2019. *Atmosphere* **2019**, *10*, 642. [CrossRef]

77. Santos, A.L.M.; Gonçalves, W.A.; Andrade, L.D.M.B.; Rodrigues, D.T.; Batista, F.F.; Lima, G.C.; Silva, C.M.S. Space–Time Characterization of Extreme Precipitation Indices for the Semiarid Region of Brazil. *Climate* **2024**, *12*, 43. [CrossRef]
78. Bezerra, H.C. *Monitoramento Hidrológico*; Boletim No 2—25 January 2012; CPRM—Serviço Geológico do Brasil: Brasília, Brazil, 2012; p. 11.
79. Espinoza, J.C.; Marengo, J.A.; Ronchail, J.; Carpio, J.M.; Flores, L.N.; Guyot, J.L. The extreme 2014 flood in south-western Amazon basin: The role of tropical-subtropical South Atlantic SST gradient. *Environ. Res. Lett.* **2014**, *9*, 124007. [CrossRef]
80. Tomasella, J.; Borma, L.S.; Marengo, J.A.; Rodriguez, D.A.; Cuartas, L.A.; Nobre, C.A.; Prado, M.C. The droughts of 1996–1997 and 2004–2005 in Amazonia: Hydrological response in the river main-stem. *Hydrol. Process.* **2011**, *25*, 1228–1242. [CrossRef]
81. Laureanti, N.C.; Tavares, P.D.S.; Tavares, M.; Rodrigues, D.C.; Gomes, J.L.; Chou, S.C.; Correia, F.W.S. Extreme Seasonal Droughts and Floods in the Madeira River Basin, Brazil: Diagnosis, Causes, and Trends. *Climate* **2024**, *12*, 111. [CrossRef]
82. Molina-Carpio, J.; Espinoza, J.C.; Vauchel, P.; Ronchail, J.; Gutierrez Caloir, B.; Guyot, J.L.; Noriega, L. Hydroclimatology of the Upper Madeira River basin: Spatio-temporal variability and trends. *Hydrol. Sci. J.* **2017**, *62*, 911–927. [CrossRef]
83. Itaipu Binacional. Chuvas provocam vazão histórica no encontro dos rios Iguaçu e Paraná. 2013. Available online: <https://www.itaipu.gov.br/sala-de-imprensa/noticia/chuvas-provocam-vazao-historica-no-encontro-dos-rios-iguacu-e-parana#:~:text=Houve%20registro%20de%20enchentes%20em,foram%20quatro%20acima%20desse%20%C3%ADndice> (accessed on 3 July 2024).
84. Fleischmann, A.S.; Siqueira, V.A.; Wongchuig-Correa, S.; Collischonn, W.; Paiva, R.C.D.D. The great 1983 floods in South American large rivers: A continental hydrological modelling approach. *Hydrol. Sci. J.* **2020**, *65*, 1358–1373. [CrossRef]
85. Cumplido, M.A.; Inocente, M.C.; Medeiros, T.P.; Oliveira, G.S.; Marengo, J.A. Secas e crises hídricas no Sudeste do Brasil: Um histórico comparativo entre os eventos de 2001, 2014 e 2021 com enfoque na bacia do rio Paraná. *Rev. Bras. Climatol.* **2023**, *32*, 129–153. [CrossRef]
86. CBHSF. RP1A —Diagnóstico da Dimensão Técnica e Institucional. In *Plano de Recursos Hídricos da Bacia Hidrográfica do rio São Francisco (2016–2025)*; CBHSF: São Paulo, Brazil, 2015; p. 318. Available online: https://2017.cbhsaofrancisco.org.br/wp-content/uploads/2015/08/V7_usos_diag_v2.pdf (accessed on 8 July 2024).
87. Marengo, J.A.; Espinoza, J.C. Extreme seasonal droughts and floods in Amazonia: Causes, trends and impacts. *Int. J. Climatol.* **2015**, *36*. [CrossRef]
88. Marengo, J.A.; Cunha, A.P.; Espinoza, J.C.; Fu, R.; Schöngart, J.; Jimenez, J.C.; Costa, M.C.; Ribeiro, J.M.; Wongchuig, S.; Zhao, S. The Drought of Amazonia in 2023–2024. *Am. J. Clim. Change* **2024**, *13*, 567–597. [CrossRef]
89. Sorí, R.; Marengo, J.A.; Nieto, R.; Drumond, A.; Gimeno, L. The atmospheric branch of the hydrological cycle over the Negro and Madeira river basins in the Amazon Region. *Water* **2018**, *10*, 738. [CrossRef]
90. Naumann, G.; Podesta, G.; Marengo, J.; Luterbacher, J.; Bavera, D.; Arias Muñoz, C.; Barbosa, P.; Cammalleri, C.; Chamorro, L.; Cuartas, A.; et al. *The 2019–2021 Extreme Drought Episode in La Plata Basin*; Publications Office of the European Union: Luxembourg, 2021.
91. Vieira, R.M.D.S.P.; Sestini, M.F.; Tomasella, J.; Marchezini, V.; Pereira, G.R.; Barbosa, A.A.; Santos, F.C.; Rodriguez, D.A.; do Nascimento, F.R.; Santana, M.O.; et al. Characterizing spatio-temporal patterns of social vulnerability to droughts, degradation and desertification in the Brazilian northeast. *Environ. Sustain. Indic.* **2020**, *5*, 100016. [CrossRef]
92. Vieira, R.M.D.S.P.; Tomasella, J.; Cunha, A.P.M.D.A.; Barbosa, A.A.; Pompeu, J.; Ferreira, Y.; Santos, F.C.; Alves, L.M.; Ometto, J. Socio-environmental vulnerability to drought conditions and land degradation: An assessment in two northeastern Brazilian river basins. *Sustainability* **2023**, *15*, 8029. [CrossRef]
93. Reboita, M.S.; Kuki, C.A.C.; Marrafon, V.H.; Souza, C.A.; Ferreira, G.W.S.; Teodoro, T.; Lima, J.W.M. South America climate change revealed through climate indices projected by GCMs and Eta-RCM ensembles. *Clim. Dyn.* **2022**, *58*, 459–485. [CrossRef]
94. Llopart, M.; Domingues, L.M.; Torma, C.; Giorgi, F.; Rocha, R.P.; Ambrizzi, T.; Reboita, M.S.; Alves, L.M.; Coppola, L.M.; da Silva, M.L.; et al. Assessing changes in the atmospheric water budget as drivers for precipitation change over two CORDEX-CORE domains. *Clim. Dyn.* **2021**, *57*, 1615–1628. [CrossRef]
95. Jones, M.W.; Veraverbeke, S.; Andela, N.; Doerr, S.H.; Kolden, C.; Mataveli, G.; Pettinari, M.L.; Le Quéré, C.; Rosan, T.M.; van der Werf, G.R.; et al. Global rise in forest fire emissions linked to climate change in the extratropics. *Science* **2024**, *386*, ead15889. [CrossRef]
96. Vicente-Serrano, S.M.; Trambly, Y.; Murphy, C.; Ocampo-Melgar, A.; Guan, H.; Spinoni, J.; Marengo, J.; Ghosh, S.; Yang, Y.; Cheval, S.; et al. First Issue of Water Scarcity and Drought. *Water Scarcity Drought* **2024**, *1*, 1–5. Available online: <https://www.sciltp.com/journals/wsd/article/view/479> (accessed on 3 July 2024).

Disclaimer/Publisher’s Note: The statements, opinions and data contained in all publications are solely those of the individual author(s) and contributor(s) and not of MDPI and/or the editor(s). MDPI and/or the editor(s) disclaim responsibility for any injury to people or property resulting from any ideas, methods, instructions or products referred to in the content.